Received: March 18, 2022. Revised: April 5, 2022.

INASS

International Journal of
Intelligent Engineering & Systems

http://www.inass.org/

Performance of Cellular Based UAM with Selective CoMP

Nam-Soo Kim[1]*

[1]*Department of Electronic Engineering, Cheongju University, Rep. of Korea*
* Corresponding author's Email: nskim@cju.ac.kr

Abstract: The non-orthogonal multiple access (NOMA), which is a power domain multiplexing technology, has received considerable attention for 5G and beyond cellular systems due to its higher spectral efficiency. Coordinated multipoint (CoMP) transmission has been adapted in NOMA systems to improve the performance of a cell edge user. Conventional CoMP combines received signals from multiple sources using maximum ratio combining (MRC) in order to improve the user's signal-to-noise ratio (SNR). While MRC provides the highest diversity gain of any diversity combining technology, it requires latency for co-phasing and combining the received signals. Recently, urban air mobility (UAM) has emerged as a viable option for future mobility in metropolitan areas in order to avoid terrestrial traffic congestion. However, a flight control information of a UAM, especially an unmanned UAM is very sensitive to latency. Hence MRC is not recommendable for UAM due to the inherent latency. We consider selection combining (SC) which has less latency rather than MRC as a combining technology in CoMP. This study derives the outage performance of UAM with selective CoMP in closed-form. The analytical results are compared and verified with that of the Monte Carlo simulation. The outage performances of a UAM in NOMA-NOMA and NOMA-OMA modes are compared. It is shown that the NOMA-OMA mode has better performance than the NOMA-NOMA mode irrespective of the given conditions, and has over 3 dB SNR gains under the given conditions. When the performance of UAM in the NOMA-NOMA mode is not satisfying, it is recommended to switch to the NOMA-OMA mode based on this study.

Keywords: Cellular network, CoMP, Link performance, NOMA, UAM.

1. Introduction

Future cellular mobile systems require fast data transmission, low latency, and high spectral efficiency. To satisfy these user requirements, non-orthogonal multiple access (NOMA) has been focused on recently [1, 2]. Also, power control for the near and far users [3], the user or dedicated relay [4, 5], and coordinated multipoint (CoMP) transmission have been actively studied for the performance enhancement of NOMA systems [6, 7].

On the other hand, the deployment of urban air mobility (UAM) is actively considered in metropolitan areas for avoiding terrestrial traffic congestions [8]. Since a UAM flying at low altitude compared to aircraft and at high speed to ground vehicles, there are high possibilities to be influenced by the shadow fading caused by the tall and high-density buildings in city areas. Consequently, the UAM with CoMP, which receives multiple information from multi-cell for better performance, has been reported [9].

Typically, the CoMP system adapts to maximal ratio combining (MRC), which increases the signal-to-interference plus noise ratio (SINR) received [10, 11]. MRC produces a weighted sum of the received signals that has been co-phased prior to combining. As a result, MRC consumes processing time, resulting in delay and increased power consumption. Due to the high speed of a UAM, low latency is critical when it comes to flight control information.

A simpler type of spatial combining such as a selection combining (SC) does not require weighting and co-phasing. Different from MRC, it selects the highest SINR among received signals, hence reducing latency and power consumption [12]. Though SC has less diversity gain, it is suitable for latency-limited systems such as UAM. The less diversity gain can be covered by the more transmitting power from a base station.

This study considers the outage probability of UAM with selective CoMP which adapts the selection combining. Two system modes are proposed; firstly, a NOMA-NOMA mode which has NOMA protocol in both cell 1 and cell 2. Secondly, a NONA-OMA mode which has NOMA protocol for cell 1 and orthogonal multiple access (OMA) protocol for cell 2. Each cell has two users, a ground user (GU) and an air user (AU) of UAM. In the NOMA-NOMA mode, the transmitting power is allocated to GU and AU. However, in the NOMA-OMA mode, the transmitting power of the OMA cell of cell 2 is allocated only to the AU. We can select the NOMA-NOMA mode or the NOMA-OMA mode for the performance improvement of the AU. The outage performances of both cases are derived in closed-form and verified to the Monte-Carlo simulation. The main contribution of this paper is the analysis of the outage performance of UAM with selective CoMP for the NOMA-NOMA and NOMA-OMA modes in closed-form. The results can be applied to decide the selection of cases for reliable UAM communication.

The rest of this paper is organized as follows. Section II describes a UAM that incorporates a selective CoMP system model, a channel model, and a received signal-to-interference plus noise ratio (SINR). Section III derives the closed-form outage probabilities for the UAM with selective CoMP which considers both two modes, namely, NOMA-NOMA and NOMA-OMA. In section IV, numerical examples of the outage probability for the two cases are presented, along with a comparison of the analytical and Monte Carlo simulation results. Finally, section V discusses the study's conclusions and future research directions.

2. System model

Fig. 1 shows a selective CoMP system model, which consists of two cells; cell 1 is NOMA cell and cell 2 is NOMA /OMA cell. There are two users, a GU and an AU in a cell. In this study, we consider a UAM as an AU. The AU receives two signals through the BS1-AU and BS2-AU links, of which channel coefficients denote g_1 and g_2, respectively. The wireless environment of an individual link is different, hence the channels are assumed independent of each other in this study.

In Fig. 1, h_1 and h_2 denote the channel coefficient of the BS1-GU1 and BS2-GU2 links, respectively. These terrestrial channel coefficients have complex Gaussian distribution with zero mean and unit variance, $h_1 \sim CN(0,1)$ and $h_2 \sim CN(0,1)$.

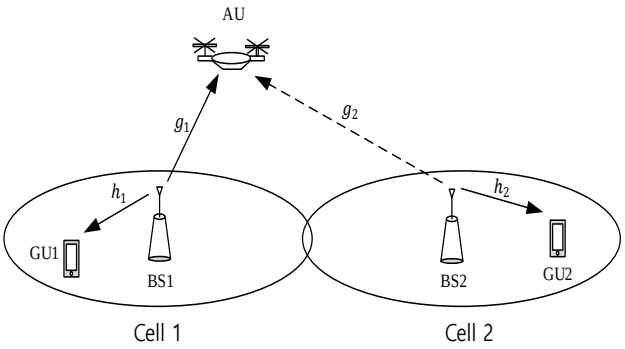

Figure. 1 Selective CoMP system model

For the notational convenience denote $H_1 = |h_1|^2$ and $H_2 = |h_2|^2$, then the probability density function (pdf), f_H, and the cumulative distribution function (CDF), F_H can be written by

$$f_{H_i}(x) = e^{-x}, F_{H_i}(x) = 1 - e^{-x}, i \in \{1,2\}. \quad (1)$$

The channel gain of the BS-GU link is denoted as

$$G_{g_i} = A_{g_i} d_{g_i}^{-\nu_g}, \; i \in \{1,2\} \quad (2)$$

where A_{g_i} is the gain constant of the BS1-GU1 and BS2-GU2 link, it is a function of the carrier frequency and antenna gain [13]. d_{g_i} is the distance between a BS and a GU, and ν_g is the ground path-loss exponent.

While g_1 and g_2 is the aerial channel coefficient of the BS1-AU and BS2-AU links, respectively. Generally, the received signal through an aerial channel consists of the direct and indirect signal components, hence it has Rician distribution. Similarly, define $G_1 = |g_1|^2$ and $G_2 = |g_2|^2$. The pdf of G_1 and G_2 is given by [14]

$$f_{G_i}(x) = \frac{(1+K)e^{-K}}{\Omega_{G_i}} e^{-(1+K)x/\Omega_{G_i}} I_0\left(2\sqrt{\frac{(1+K)Kx}{\Omega_{G_i}}}\right), \; i\epsilon\{1,2\} \quad (3)$$

where Ω_{G_i} is the average of G_i, let G_i equals 1. And the CDF of G_1 and G_2 can be written by

$$F_{G_i}(x) = 1 - Q\left(\sqrt{2K}, \sqrt{2(1+K)x}\right), \; i\epsilon\{1,2\} \quad (4)$$

where K is the Rician factor which is the ratio of the direct signal power-to-indirect signal power. And $Q(a, b)$ is the Marcum Q function [15],

$$\mathrm{Q(a,b)} = e^{-a^2/2} \sum_{k=0}^{\infty} \left(\frac{1}{k!}\right)^2 \left(\frac{a^2}{2}\right)^k \Gamma\left(1+k, \frac{b^2}{2}\right) \quad (5)$$

where [16]

$$\Gamma(1+n, x) = n!\, e^{-x} \sum_{m=0}^{n} \frac{x^m}{m!} \quad . \quad (6)$$

Meanwhile, there is a relation between the Rician factor K and altitude angle θ [17],

$$K = K_{min}\, exp\left\{\frac{2}{\pi} ln\left(\frac{K_{max}}{K_{min}}\theta\right)\right\} \quad (7)$$

where K_{min} and K_{max} are the Rician factors of $\theta = 0$ and $\theta = \pi/2$ [rad], respectively [18, 19].

The channel gain G_{a_i} of the BS-AU link is given by

$$G_{a_i} = A_{a_i} d_{a_i}^{-\nu_a} \quad (8)$$

where A_{a_i} is the gain constant of the BS-AU link. d_{a_i} denotes the distance between a BS and an AU, and ν_a is the aerial path-loss exponent.

Generally, NOMA system multiplexes users in a cell with different power levels such as for the weak user which has less channel gain is allocated more power and vice versa.

The transmitted signal from BS1 is $\left(\sqrt{P_1\alpha_{s1}}x_{s1} + \sqrt{P_1\alpha_{w1}}x_{w1}\right)$ where P_1 is the transmit power from BS1. And α_{s1} and α_{w1} are power allocation coefficients for the strong user and the weak user, respectively, with $\alpha_{s1} + \alpha_{w1} = 1$. x_{s1} and x_{w1} are the information of the strong user and weak user, respectively. The information has bipolar and square mean equals one, i.e., $E[|x_{s1}|^2] = E[|x_{w1}|^2] = 1$, where E[·] denotes expectation.

When cell 2 operates in NOMA mode, the transmitted signal from BS2 is $\left(\sqrt{P_2\alpha_{s2}}x_{s2} + \sqrt{P_2\alpha_{w2}}x_{w2}\right)$ where P_2 is the transmit power from BS2. Similarly, α_{s2} and α_{w2} are power allocation coefficients for the strong user and the weak user, respectively, with $\alpha_{s2} + \alpha_{w2} = 1$. x_{s2} and x_{w2} are the information of the strong user and weak user, respectively, with $E[|x_{s2}|^2] = E[|x_{w2}|^2] = 1$.

The received signal of UAM from the BS1-AU link can be written by

$$y_{A1} = g_1\sqrt{P_1 G_{a1}}\left(\sqrt{\alpha_{s1}}x_{s1} + \sqrt{\alpha_{w1}}x_{w1}\right) + n_A \quad (9)$$

where n_A is the white noise of UAM with zero mean and unit variance of N_0, $n_A \sim CN(0, N_0)$. Similarly, the received signal of UAM from the BS2-AU link is

$$y_{A2,NOMA} = g_2\sqrt{P_2 G_{a2}}\left(\sqrt{\alpha_{s2}}x_{s2} + \sqrt{\alpha_{w2}}x_{w2}\right) + n_A \, . \quad (10)$$

When cell 2 operates in OMA mode, BS2 transmits $\sqrt{P_2}x_a$ that is AU signal only. x_a becomes x_{s1} or x_{w1} when UAM is a strong or weak user of BS1, respectively. The received signal of UAM from the BS2-AU link is given by

$$y_{A2,OMA} = g_2\sqrt{P_2 G_{a2}}x_a + n_A \, . \quad (11)$$

In a NOMA system, the strong signal is decoded first, and the weak signal is decoded after removing the strong interference with successive interference cancellation (SIC). Therefore, the received SINR of UAM, γ_1, from BS1 becomes

$$\gamma_1 = \begin{cases} \frac{\rho_1 G_1 G_{a1}\alpha_{w1}}{\rho_1 G_1 G_{a1}\alpha_{s1}+1} & , \; G_{g1}H_1 > G_{a1}G_1 \\ \rho_1 G_1 G_{a1}\alpha_{s1} & , \; G_{g1}H_1 \le G_{a1}G_1 \end{cases} \quad (12)$$

where the transmit signal-to-noise ratio (SNR) of ρ_1 defines $\rho_1 = P_1/N_o$. Similarly, the SINR of UAM from BS2 of NOMA cell 2, $\gamma_{2,NOMA}$, is

$$\gamma_{2,NOMA} = \begin{cases} \frac{\rho_2 G_2 G_{a2}\alpha_{w2}}{\rho_2 G_2 G_{a2}\alpha_{s2}+1} & , \; G_{g2}H_2 > G_{a2}G_2 \\ \rho_2 G_2 G_{a2}\alpha_{s2} & , \; G_{g2}H_2 \le G_{a2}G_2 \end{cases} \quad (13)$$

where ρ_2 denotes $\rho_2 = P_2/N_0$ which is the transmit SNR of BS2.

When BS2 operates in OMA mode, all the transmission power is allocated to the AU, and no power is assigned to the GU in cell 2. Then the received SINR at UAM, $\gamma_{2,OMA}$ is given by

$$\gamma_{2,OMA} = \rho_2 G_2 \, . \quad (14)$$

According to the selection combining rules of SC, the UAM selects the stronger signal between the signals from BS1 and BS2, and the selected SINR can be written by

$$\gamma_{A,i} = max\{\gamma_1, \gamma_{2,i}\}, i \in \{NOMA, OMA\} \, . \quad (15)$$

3. Outage probability

An outage event happens when the received SINR γ_A at UAM bellows threshold, then the outage probability is given by

$$P_0 = Pr(\gamma_A < \Gamma) \quad (16)$$

where Γ is the threshold, $\Gamma = 2^R - 1$ where R is the

spectral efficiency in [bps/Hz]. By applying Eq. (15) into Eq. (16), the outage probability of the selective CoMP system can be written by [10]

$$\begin{aligned} P_{0,i} &= Pr(\gamma_{A,i} < \Gamma) \\ &= Pr(\gamma_1 < \Gamma) \times Pr(\gamma_{2,i} < \Gamma) \\ &= P_{01} \times P_{02,i}\,, \quad i \in \{NOMA, OMA\} \end{aligned} \tag{17}$$

where the second equality assumes that the individual channels are independent of each other. Also P_{01} and $P_{02,i}$ define $P_{01} = Pr(\gamma_1 < \Gamma)$ and $P_{02,i} = Pr(\gamma_{2,i} < \Gamma)$, respectively. $P_{02,NOMA}$ and $P_{02,OMA}$ denote the outage probability of a UAM that cell 2 operates in NOMA mode or OMA mode, respectively.

3.1 Outage probability of NOMA-NOMA mode

When both cells operate in NOMA mode, the NOMA-NOMA mode, the outage probability of P_{01} in Eq. (17) is

$$\begin{aligned} &P_{01} = \\ &Pr(G_1 < \xi_1 | G_{g1}H_1 > G_{a1}G_1) Pr(G_{g1}H_1 > G_{a1}G_1) \\ &\qquad + \\ &Pr(G_1 < \xi_2 | G_{g1}H_1 \le G_{a1}G_1) Pr(G_{g1}H_1 \le G_{a1}G_1), \\ &\alpha_{w1} > \Gamma\alpha_{s1} \end{aligned} \tag{18}$$

where ξ_1 and ξ_2 are $\xi_1 = \Gamma/\rho_1 G_{a1}(\alpha_{w1} - \Gamma\alpha_{s1})$ and $\xi_2 = \Gamma/\rho_1 G_{a1}\alpha_{s1}$, respectively. By applying Eq. (4) into Eq. (18), the first probability in Eq. (18) can be written by

$$\begin{aligned} &Pr(G_1 < \xi_1 | G_{g1}H_1 > G_{a1}G_1) \\ &= 1 - Q\left(\sqrt{2K}, \sqrt{2(1+K)\xi_1}\right) \\ &= 1 - e^{-\{K+(1+K)\xi_1\}} \sum_{k=0}^{\infty} \frac{K^k}{k!} \sum_{m=0}^{k} \frac{(1+K)^m}{m!} \xi_1^m \end{aligned} \tag{19}$$

where the second equality is obtained from Eq. (5).

Similarly, the third probability in Eq. (18) becomes

$$\begin{aligned} &Pr(G_1 < \xi_2 | G_{g1}H_1 \le G_{a1}G_1) \\ &= 1 - Q\left(\sqrt{2K}, \sqrt{2(1+K)\xi_2}\right) \\ &= 1 - e^{-\{K+(1+K)\xi_2\}} \sum_{k=0}^{\infty} \frac{K^k}{k!} \sum_{m=0}^{k} \frac{(1+K)^m}{m!} \xi_2^m. \end{aligned} \tag{20}$$

The second probability in Eq. (18) is

$$\begin{aligned} Pr(G_{g1}H_1 > G_{a1}G_1) &= Pr\left(G_1 < H_1 \frac{G_{g1}}{G_{a1}}\right) \\ &= 1 - \int_0^{\infty} Q\left(\sqrt{2K}, \sqrt{2(1+K)\frac{G_{g1}}{G_{a1}}x}\right) e^{-x} dx. \end{aligned} \tag{21}$$

Replacing Eq. (21) with Eq. (5), the probability of Eq. (21) can be rearranged by [16, 20]

$$\begin{aligned} &Pr(G_{g1}H_1 > G_{a1}G_1) \\ &= 1 - e^{-K} \sum_{k=0}^{\infty} \frac{K^k}{k!} \sum_{m=0}^{k} \frac{(1+K)^m (G_{a1}/G_{g1})}{(1+K+G_{a1}/G_{g1})^{m+1}}. \end{aligned} \tag{22}$$

The fourth probability in Eq. (18) is given by

$$Pr(G_{g1}H_1 \le G_{a1}G_1) = 1 - Pr(G_{g1}H_1 > G_{a1}G_1). \tag{23}$$

Similar to Eq. (18), the probability of $P_{02,NOMA}$ in Eq. (17) with NOMA mode can be obtained by

$$\begin{aligned} &P_{02,NOMA} = \\ &Pr(G_2 < \xi_3 | G_{g2}H_2 > G_{a2}G_2) Pr(G_{g2}H_2 > G_{a2}G_2) \\ &\qquad + \\ &Pr(G_2 < \xi_4 | G_{g2}H_2 \le G_{a2}G_2) Pr(G_{g2}H_2 \le G_{a2}G_2), \\ &\alpha_{w2} > \Gamma\alpha_{s1} \end{aligned} \tag{24}$$

where $\xi_3 = \Gamma/\rho_2 G_{a2}(\alpha_{w2} - \Gamma\alpha_{s2})$ and $\xi_4 = \Gamma/\rho_2 G_{a2}\alpha_{s2}$. In the same manner of Eq. (19), the first probability of Eq. (24) can be written by

$$\begin{aligned} &Pr(G_2 < \xi_3 | G_{g2}H_2 > G_{a2}G_2) \\ &= 1 - e^{-\{K+(1+K)\xi_3\}} \sum_{k=0}^{\infty} \frac{K^k}{k!} \sum_{m=0}^{k} \frac{(1+K)^m}{m!} \xi_3^m. \end{aligned} \tag{25}$$

The third probability of Eq. (24) can be obtained from Eq. (20) similarly,

$$\begin{aligned} &Pr(G_2 < \xi_4 | G_{g2}H_2 \le G_{a2}G_2) \\ &= 1 - e^{-\{K+(1+K)\xi_4\}} \sum_{k=0}^{\infty} \frac{K^k}{k!} \sum_{m=0}^{k} \frac{(1+K)^m}{m!} \xi_4^m. \end{aligned} \tag{26}$$

Also, the second probability of Eq. (24) derived from Eq. (22),

$$\begin{aligned} &Pr(G_{g2}H_2 > G_{a2}G_2) \\ &= 1 - e^{-K} \sum_{k=0}^{\infty} \frac{K^k}{k!} \sum_{m=0}^{k} \frac{(1+K)^m (G_{a2}/G_{g2})}{(1+K+G_{a2}/G_{g2})^{m+1}}. \end{aligned} \tag{27}$$

The fourth probability of Eq. (24) was also obtained from Eq. (27),

$$Pr(G_{g2}H_2 \le G_{a2}G_2) = 1 - Pr(G_{g2}H_2 > G_{a2}G_2). \tag{28}$$

3.2 Outage probability of NOMA-OMA mode

When cell 1 operates in NOMA mode and cell 2 operates in OMA mode, the NOMA-OMA mode, the second outage probability of $P_{02,OMA}$, in Eq. (17) becomes

$$P_{02,OMA} = Pr(\gamma_{2,OMA} < \Gamma) = Pr(G_2 < \xi_{OMA}) \tag{29}$$

where the second equality is obtained from Eq. (14) and $\xi_{OMA} = \Gamma/\rho_2 G_{a2}$. By replacing ξ_3 of Eq. (25) with ξ_{OMA}, $P_{02,OMA}$ can be obtained. Hence, the outage probability of UAM in the NOMA-OMA mode can be written by

$$P_{0,OMA} = P_{01} \times P_{02,OMA} \tag{30}$$

where P_{01} is given in Eq. (18).

4. Numerical examples

In this section, the outage probabilities of UAM in NOMA-NOMA CoMP and the NOMA-OMA CoMP modes are analyzed. And the analytical results are compared with that of the simulation. For the numerical examples, we assumed $G_{a1} = G_{a2} = G_{g1} = G_{g2}$=1, α_{w1}=α_{w2}=0.8 in the NOMA-NOMA mode. In the NOMA-OMA mode, there is no transmit power to GU2, hence, we assumed $G_{a1} = G_{a2} = G_{g1}$= 1, α_{w1} = 0.8. Monte-Carlo simulation results are obtained through 1×10^7 trials.

Fig. 2 shows the outage probability of UAM as a function of SINR where "*" indicates simulation results. The solid line and the partial line show the NOMA-NOMA mode and NOMA-OMA mode, respectively. It shows that the analysis and simulation results are matched well, which means the analysis is exact.

For comparison, the no CoMP mode is also shown. In the no CoMP mode, UAM only receives from the BS 1, hence it shows poorer performance than CoMP modes. The required SNR to maintain the outage probability of 1×10^{-3} is 34 dB, 28.5 dB, and 18.9 dB for $K = 1$, $K = 3$, and $K = 7$, respectively, in the no CoMP mode. However, that is 19 dB, 15.1 dB, and 11.9 dB in the NOMA-NOMA mode. Less power is required which means SNR gains can be obtained.

As the Rician factor increases, the power of the direct path increases, hence, the outage probability decreases. It is noticed that the SNR gain, which maintains the identical outage probability, does not proportional to the increase of the Rician factor.

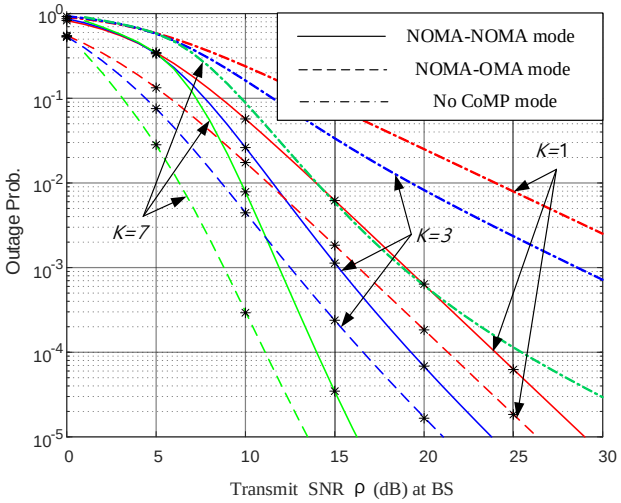

Figure. 2 Outage probability of UAM with different Rician factors ($R = 1, \rho_1 = \rho_2 = \rho$)

When the Rician factor is given in Fig. 2, the transmit SNR of the NOMA-OMA mode to hold the outage probability of 1×10^{-3} is less than about 3 dB compared to the NOMA-NOMA mode. It is interpreted that the NOMA-OMA mode always has better performance than the NOMA-NOMA mode. In the case of the NOMA-NOMA mode, the transmit power of BS2 is divided into the GU2 and AU. However, the transmit power of the BS2 is allocated to the AU only in the NOMA-OMA mode.

The outage probability becomes 7.8×10^{-3} and 2.9×10^{-4} in the NOMA-NOMA and NOMA-OMA mode, respectively, when Rician factor, $K = 7$, and SNR = 10 dB in Fig. 2. It also shows the NOMA-OMA mode has better performance than the NOMA-NOMA mode.

In a NOMA system, the performance depends on the power allocation to users. Fig. 3 shows the performance of UAM is subject to power allocation. It shows that the minimum outage probability holds around the power allocation coefficient of 0.7 to the weak user in cell 1, which operates in the NOMA protocol. Similar to the trend of Fig. 2, it shows the outage probability decreases as the increase of Rician factor. In the same manner, the NOMA-OMA mode has a better performance than the NOMA-NOMA mode.

The effect of the elevation angle on the outage probability of UAM is shown in Fig. 4. The analytical results agree well with that of the simulation. According to the rise of the elevation angle, the Rician factor increases, and eventually, the outage probability decreases.

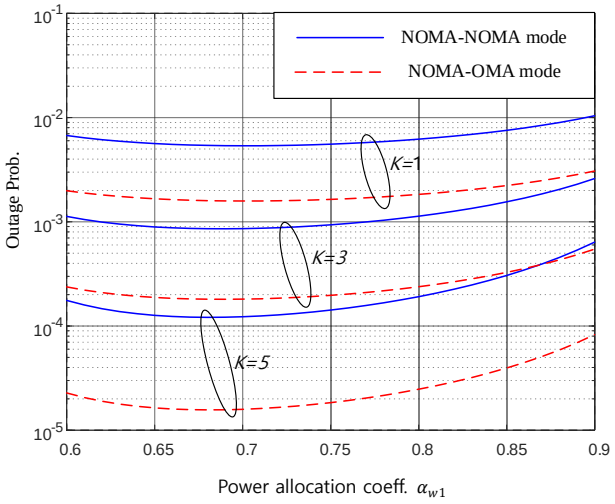

Figure. 3 Outage probability of UAM vs. power allocation $(R = 1, \rho_1 = \rho_2 = \rho)$

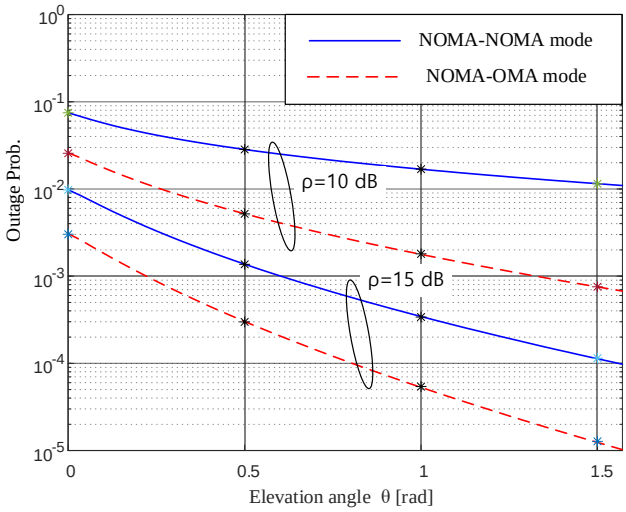

Figure. 4 Outage probability of UAM vs. elevation angle $(R = 1, K_{min} = 1,\ K_{max} = 10,\ \rho_1 = \rho_2 = \rho)$

5. Conclusions

This paper considered the outage probability of a UAM with selective CoMP. Since a UAM travels with high speed than a terrestrial automobile, it is more susceptible to severe shadowing caused by the urban propagation environment. It was assumed that a UAM is located at the cell edge and enhanced performance using CoMP technology. In addition, the selective CoMP system was adapted in particular for low latency and fast processing. We have proposed two modes, the NOMA-NOMA and NOMA-OMA modes which adapt CoMP. And the outage probability of a UAM with the NOMA-NOMA mode and the NOMA-OMA mode has been derived in closed-form. The analytical results were verified through Monte Carlo simulation with 1×10^7 trials.

As we expected, the NOMA-OMA mode obtained better performance than the NOMA-NOMA mode, i.e., over 3 dB SNR gain at the given conditions. When the power allocation coefficient of 0.7 for the weak user in cell 1, the best performance is obtained irrespective of the NOMA-NOMA or NOMA-OMA modes. Also, the outage performance decreased with the increase of the elevation angle. We have noticed that the proposed two modes always have better performance than no CoMP mode.

From the obtained results, the NOMA-OMA mode had better performance than the NOMA-NOMA mode. However, it is generally accepted that the spectral efficiency of OMA is smaller than that of NOMA.

Therefore, we can conclude that though the NOMA-OMA mode has less spectral efficiency, it can provide more reliable communication for UAM than the OMA-NOMA mode. Further study will be focused on the latency and the performance enhancement of UAM.

Conflicts of interest

The authors declare no conflict of interest.

References

[1] Z. Wu, K. Lu, C. Jiang, and X. Shao, "Comprehensive study and comparison on 5G NOMA schemes", *IEEE Access*, Vol. 6, pp. 18511-18519, 2018.

[2] B. Makki, K. Chitti, A. Behravan, and M. S. Alouini, "A survey of NOMA: Current status and open research challenges", *IEEE Open Journal of the Communications Society*, Vol. 1, pp. 179-189, 2020.

[3] H. Zhang, B. Wang, C. Jiang, K. Long, V. Leung, and H. V. Poor, "Energy efficient dynamic resource optimization in NOMA systems", *IEEE Transactions on Wireless Communications*, Vol. 17, No. 9, pp. 5671-5683, 2018.

[4] Q. Y. Liau and C. Y. Leow, "Successive user relaying in cooperative NOMA system", *IEEE Wireless Communications Letters*, Vol. 8, No. 3, pp. 921-924, 2019.

[5] N. S. Kim, "Overlay Cognitive Radio NOMA Networks with Selected Relay and Direct Link", *International Journal of Intelligent Engineering and Systems*, Vol. 13, No. 1, pp. 181-190, 2020, doi: 10.22266/ijies2020.0229.17.

[6] Y. Sun, Z. Ding, X. Dai, and O. A. Dobre, "On the performance of network NOMA in uplink CoMP systems: A stochastic geometry approach", *IEEE Transactions on Communications*, Vol. 67, No. 7, pp. 5084-5098, 2019.

[7] J. Chen, Y. Xie, X. Mu, J. Jia, Y. Liu, and X. Wang, "Energy efficient resource allocation for IRS assisted CoMP systems", *IEEE Transactions on Communications*, Early access article, 2022.
DOI: 10.1109/TWC.2022.3142784.

[8] X. Yang, L. Deng, J. Liu, P. Wei, and H. Li, "Multi-agent autonomous operations in urban air mobility with communication constraints", In: *Proc. of American Institute of Aeronautics and Astronautics* (AIAA) SciTech Forum, Orlando, FL, 2020.

[9] L. Liu, S. Zhang, and R. Zhang, "CoMP in the sky: UAV placement and movement optimization for multi-user communications", *IEEE Transactions on Communications*, Vol. 67, No. 8, pp. 5645-5658, 2019.

[10] A. Goldsmith, *Wireless Communications*, Cambridge University Press, New York, 2005.

[11] Y. Zhao, W. Li, Y. Gao, L. Feng, and P. Yu, "3D deployment and user association of CoMP-assisted multiple aerial base stations for wireless network capacity enhancement", In: *Proc. of International Conference on Network and Service Management*, Izmir, Turkey, 2021.

[12] C. M. Mueller, "When CoMP beneficial-and when it is not. Selective coordination from a spectral efficiency and a users' throughput perspective", In: *Proc. of IEEE Wireless Communications and Networking Conference*, Paris, France, 2012.

[13] W. K. New, C. Y. Leow, K. Navaie, and Z. Ding, "Robust non-orthogonal multiple access for aerial and ground users", *IEEE Transactions on Wireless Communications*, Vol. 19, No. 7, pp. 4793-4805, 2020.

[14] M. K. Simon and M. S. Alouini, "Digital communication over fading channels", *John Wiley&Sons, New York*, N. Y. 2000.

[15] A. Annamalai, C. Tellambura, and J. Matyjas, "A new twist on the generalized Marcum Q-function with fractional-order M and its applications", In: *Proceedings of IEEE Consumer Communications and Networking Conference*, Las Vegas, NV, 2009.

[16] I. S. Gradshteyn and I. M. Ryzbik, "Table of integrals, series, and products", *6th Ed., Academic Press*, 2002.

[17] M. M. Azari, F. Rosas, K. C. Chen, and S. Pollin, "Ultra reliable UAV communication using altitude and cooperation diversity", *IEEE Transactions on Communications*, Vol. 66, No. 1, pp. 330-344, 2018.

[18] X. Yuan, Z. Feng, W. Xu, W. Ni, J. A. Zhang, Z. Wei, and R. P. Liu, "Capacity analysis of UAV communications: cases of random trajectories", *IEEE Transactions on Vehicular Technology*, Vol. 67, No. 8, pp. 7564-7576, 2018.

[19] M. M. Azari, F. Rosas, K. C. Chen, and S. Pollin, "Ultra reliable UAV communication using altitude and cooperation diversity", *IEEE Transactions on Communications*, Vol. 66, No. 1, pp. 330-344, 2018.

[20] N. S. Kim, "Link balance and performance of UAM in NOMA-based cellular networks", *International Journal of Intelligent Engineering and Systems*, Vol. 15, No. 1, pp. 490-498, 2022, doi: 10.22266/ijies2022.0228.44.